# Mitochondrial methionyl *N*-formylation affects steady-state levels of oxidative phosphorylation complexes and their organization into supercomplexes

Received for publication, May 6, 2018, and in revised form, August 2, 2018 Published, Papers in Press, August 7, 2018, DOI 10.1074/jbc.RA118.003838

**Tania Arguello**[‡1], **Caroline Köhrer**[§2], **Uttam L. RajBhandary**[§], **and Carlos T. Moraes**[‡3]

*From the* [‡]*Department of Neurology, University of Miami School of Medicine, Miami, Florida 33136 and* [§]*Department of Biology, Massachusetts Institute of Technology, Cambridge, Massachusetts 02139*

Edited by Ronald C. Wek

**N-Formylation of the Met-tRNA$^{Met}$ by the nuclearly encoded mitochondrial methionyl-tRNA formyltransferase (MTFMT) has been found to be a key determinant of protein synthesis initiation in mitochondria. In humans, mutations in the *MTFMT* gene result in Leigh syndrome, a progressive and severe neurometabolic disorder. However, the absolute requirement of formylation of Met-tRNA$^{Met}$ for protein synthesis in mammalian mitochondria is still debated. Here, we generated a *Mtfmt*-KO mouse fibroblast cell line and demonstrated that *N*-formylation of the first methionine via fMet-tRNA$^{Met}$ by MTFMT is not an absolute requirement for initiation of protein synthesis. However, it differentially affected the efficiency of synthesis of mtDNA-coded polypeptides. Lack of methionine *N*-formylation did not compromise the stability of these individual subunits but had a marked effect on the assembly and stability of the OXPHOS complexes I and IV and on their supercomplexes. In summary, *N*-formylation is not essential for mitochondrial protein synthesis but is critical for efficient synthesis of several mitochondrially encoded peptides and for OXPHOS complex stability and assembly into supercomplexes.**

In mitochondria, synthesis of proteins requires tightly coordinated communication between nuclear and mitochondrial DNA. Although the majority of proteins required for the process are encoded in the nuclear DNA, translated in the cytoplasm, and imported to mitochondria (1), 13 proteins that are catalytic subunits of the oxidative phosphorylation (OXPHOS)[4] system are synthesized inside mitochondria. These proteins are encoded by the mammalian mitochondrial DNA (mtDNA) along with 22 tRNAs and two ribosomal rRNAs required for their synthesis.

The current model of mitochondrial protein synthesis is divided into three conserved steps as it occurs in cytoplasm: initiation, elongation, and termination. In mammalian mitochondria, the initiation step acts as a major checkpoint and rate-limiting factor in protein synthesis (2). The nuclearly encoded protein methionyl-tRNA formyltransferase (MTFMT) is responsible for adding a formyl group to a portion of the single mitochondrial Met-tRNA$^{Met}$ (3). Once the Met-tRNA is acylated/aminoacylated with methionine (Met-tRNA$^{Met}$) and *N*-formylated by MTFMT (fMet-tRNA$^{Met}$), it is recognized by the initiation factor mtIF2 (a translational GTPase) before it binds to the small mitoribosomal subunit (SSU)–mRNA complex (2, 3). Following this, hydrolysis of GTP into GDP facilitates the binding of the large mitoribosomal subunit (LSU) and completes the formation of the initiation complex allowing elongation to start (4).

Although *N*-formylation is considered a requirement for initiation of protein synthesis in mitochondria and most bacteria, it cannot be easily generalized across species or domains of life. For example, in different bacterial species, the absence of *N*-formylation has been shown to strongly impair cellular growth (*Escherichia coli*) (5), reduce viability (*Streptococcus pneumoniae*, *Mycobacterium smegmatis*, and *Mycobacterium bovis*) (6), or have only minor effects in others (*Pseudomonas aeruginosa*) (7). In lower eukaryotes such as *Saccharomyces cerevisiae*, *N*-formylation is not essential (8). In humans, different compound heterozygous mutations in MTFMT were identified in a subset of patients diagnosed with Leigh syndrome, a severe neurometabolic disorder combined with OXPHOS dysfunction (9–15), demonstrating that *N*-formylation is critical for OXPHOS function. Furthermore, studies in fibroblasts of patients harboring mutations in the *MTFMT* gene showed reduced activity of complex I and/or IV and in some cases complex V, supporting the critical role of *N*-formylation for mitochondrial OXPHOS function.

This work was supported in part by National Institutes of Health Grants 5R01EY010804, 1R01AG036871, and 1R01NS079965 (to C. T. M.) and GM17151 (to U. L. R.). The authors declare that they have no conflicts of interest with the contents of this article. The content is solely the responsibility of the authors and does not necessarily represent the official views of the National Institutes of Health.

This article contains Figs. S1–S6.

[1] Supported by a minority supplement to National Institutes of Health Grant 5R01EY010804.

[2] Present address: Moderna Therapeutics, Cambridge, MA 02139.

[3] To whom correspondence should be addressed: Dept. of Neurology, University of Miami School of Medicine, 1420 NW 9th Ave., Miami, FL 33136. Tel.: 305-243-5858; E-mail: cmoraes@med.miami.edu.

[4] The abbreviations used are: OXPHOS, oxidative phosphorylation; MTFMT, methionyl-tRNA formyltransferase; KO, knockout; mtDNA, mitochondrial DNA; CO, cytochrome *c* oxidase; CMV, cytomegalovirus; CYTB, cytochrome *b*; SDHA, succinate dehydrogenase complex flavoprotein subunit A; UQCRC1, ubiquinol-cytochrome *c* reductase core protein I; ATP5A, ATP synthase subunit $\alpha$; BN, blue native; OCR, oxygen consumption rate; ECAR, extracellular acidification rate; CTR, control; Bis-Tris, 2-[bis(2-hydroxyethyl)amino]-2-(hydroxymethyl)propane-1,3-diol; Tricine, *N*-[2-hydroxy-1,1-bis(hydroxymethyl)ethyl]glycine; ANOVA, analysis of variance; CI, complex I, CIII, complex III; CIV, complex IV.

MTFMT expression is required for the *N*-formylation of mitochondrial Met-tRNA$^{Met}$ in patients, but there is still controversy about the absolute requirements of *N*-formylation for mitochondrial protein synthesis. Four compound heterozygous patients studied sharing the common c.626C→T mutation allele in the *MTFMT* gene showed absence of MTFMT protein expression levels (9, 13, 14) and no detectable levels of mitochondrial fMet-tRNA$^{Met}$ (9, 13). However, all mutant fibroblasts still had mitochondrial protein synthesis, albeit at decreased efficiency.

Contradictory results were also described for the *N*-formylation of COI, a mitochondrially encoded subunit of complex IV. In one study, using mutant MTFMT fibroblasts, most of the COI was not assembled into complex IV and was not *N*-formylated, suggesting that *N*-formylation of COI is required for assembly into complex IV (13). However, this finding contrasts with a previous study where, in the absence of detectable levels of MTFMT expression, *N*-formylation of COI was still observed (9).

The c.626C→T mutation is not only predicted to eliminate two exon splicing enhancers, resulting in a nonfunctional protein (9), but also a missense mutation and a.S209L substitution. The authors suggested that residual activity of the S209L mutant MTFMT protein (16) could explain the observed mitochondrial protein synthesis and the detection of *N*-formylated COI found in one study (9).

To clarify the function of MTFMT in mammals, we generated a complete *Mtfmt* knockout (KO) in mouse fibroblasts to determine whether *N*-formylation on Met-tRNA$^{Met}$ by MTFMT is an absolute requirement for protein synthesis initiation in mammalian mitochondria. We also evaluated the effects of complete ablation of *Mtfmt* on the synthesis and stability of the 13 mitochondrially encoded proteins, individual OXPHOS complexes, and their association into supercomplexes.

## Results

### *Mtfmt homozygous knockout fibroblasts do not express MTFMT protein*

To generate a complete *Mtfmt*-KO model *ex vivo*, we deleted the exon 4 of the *Mtfmt* gene in mouse skin fibroblasts using the cre-loxP technology (17). Exon 4 flanked by loxP sites was deleted using a plasmid expressing cre recombinase under the control of the CMV promoter. Deletion of exon 4 is predicted to result in the synthesis of a truncated protein. Exon 4 is present in all transcript isoforms and is where the most frequent disease mutation (c.626C→T) has been found in patients with mutations in the *MTFMT* gene. After clonal selection and expansion, we confirmed the successful deletion of exon 4 by amplification of the deleted fragment by short PCR in the *Mtfmt*-KO fibroblast clones and the absence of this fragment in the parental loxP/loxP clone (Fig. 1*A*). We did not detect MTFMT by Western blotting using enriched mitochondrial crude extracts in different *Mtfmt*-KO fibroblast clones ($n = 3$) (Fig. 1*B*). These observations confirmed the generation of a complete *Mtfmt*-knockout model in mouse fibroblasts. KO cells grew normally in enriched high-glucose medium, and gross mitochondrial distribution (by MitoTracker staining) also appeared similar to controls (not shown).

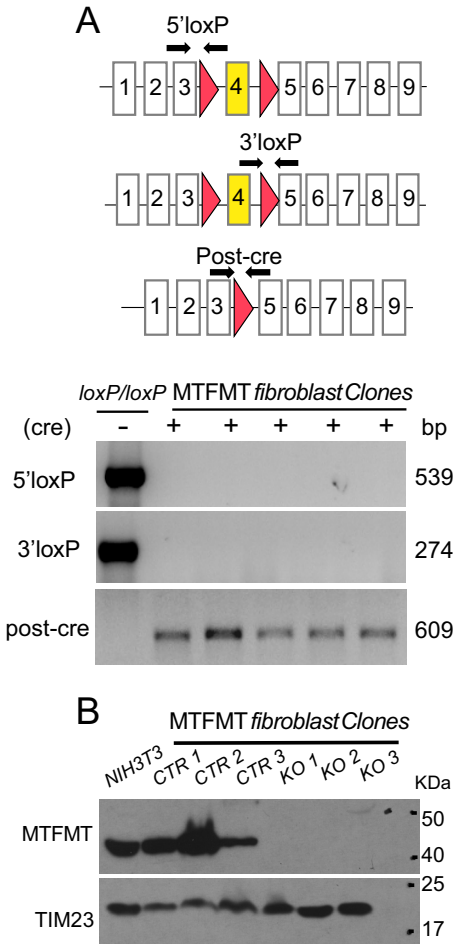


**Figure 1. *Mtfmt* homozygous knockout fibroblasts do not express MTFMT protein.** *A*, generation of the *Mtfmt*-KO mouse skin-derived fibroblast model using cre-loxP technology. Exon 4 flanked by loxP sites (5′ loxP and 3′ loxP; *red triangles*) in a parental clone (loxP/loxP) was removed by transfection with a plasmid expressing cre and confirmed by PCR amplification using specific primers (*black arrows*). Positive clones (+) with exon 4 deleted result in a putative fragment of 609 bp and no retention of 5′ (539-bp) and 3′ loxP (274-bp) amplicons. *B*, Western blotting of crude mitochondrially enriched fractions. *Mtfmt*-KO cells ($n = 3$) showed absence of MTFMT. TIM23 was used as mitochondrial loading control, and NIH3T3 mouse fibroblast cells served as a positive control of MTFMT expression.

### *Mitochondrial MTFMT is responsible for N-formylation of the Met-tRNA$^{Met}$ in mammalian mitochondria*

In mammalian mitochondria, once the unique tRNA$^{Met}$ is acylated/aminoacylated by the methionyl-tRNA synthetase, the MTFMT adds a formyl group to a portion of Met-tRNA$^{Met}$. To evaluate the activity of the MTFMT, we measured the steady-state levels of the three forms of the mitochondrial tRNA$^{Met}$: deacylated (tRNA$^{Met}$), aminoacylated (Met-tRNA$^{Met}$), and aminoacylated and *N*-formylated (fMet-tRNA$^{Met}$). These were identified by high-resolution Northern blot analysis using the cytoplasmic (Met-tRNA$_i^{Met}$) as a negative control of *N*-formylation. After isolation of total RNA under acidic conditions to maintain both Met-tRNA$^{Met}$ and fMet-tRNA$^{Met}$, we detected the three forms of tRNA$^{Met}$ in the *Mtfmt* control clones (Fig. 2*A*), which showed lower amounts of

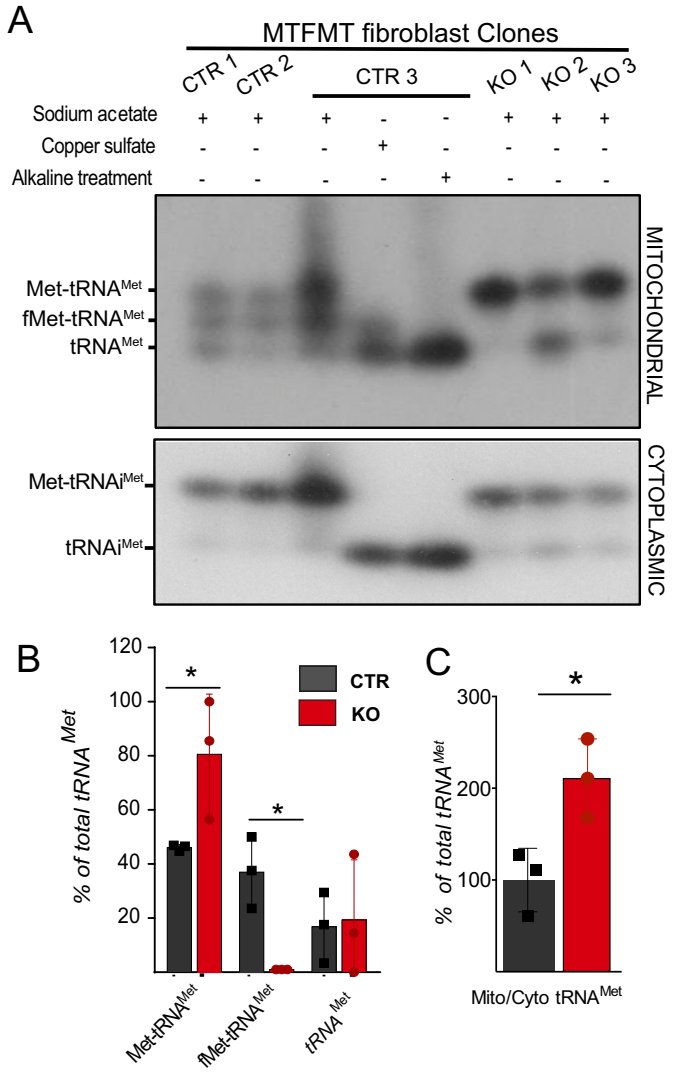


**Figure 2. Mitochondrial MTFMT is responsible for *N*-formylation of the Met-tRNA$^{Met}$ in mammalian mitochondria.** *A*, analysis of tRNAs by acid-urea PAGE allows the separation of the three forms of tRNA$^{Met}$ in RNA extracted under acidic conditions (sodium acetate). Treatment with copper sulfate deacylates only Met-tRNA$^{Met}$, allowing the visualization of fMet-tRNA$^{Met}$. Alkaline treatment deacylates both fMet-tRNA$^{Met}$ and Met-tRNA$^{Met}$, allowing the visualization of the total levels of tRNA$^{Met}$. Absence of *N*-formylation in *Mtfmt*-KO clones compared with control cell clones and preferential accumulation of the Met-tRNA$^{Met}$ are shown in the *upper panel*. Cytoplasmic initiator methionine tRNA (tRNA$_i^{Met}$) was used as an internal control (*bottom panel*). *B*, quantification of the three forms of tRNA$^{Met}$, expressed as a percentage of control and presented as the mean with *error bars* representing ±S.D. Unpaired two-way ANOVA was used for statistics (*, $p < 0.05$; $n = 3$). *C*, quantification of total mitochondrial tRNA$^{Met}$ in *Mtfmt*-KO clones, expressed as the ratio of mitochondrial (*Mito*) tRNA$^{Met}$ over cytoplasmic (*Cyto*) initiator tRNA$_i^{Met}$ with *Mtfmt* control samples set to 100% (*, $p < 0.0256$).

the deacylated tRNA$^{Met}$ form and almost equal amounts of fMet-tRNA$^{Met}$ and Met-tRNA$^{Met}$ (Fig. 2*B*). In contrast, in the *Mtfmt*-KO fibroblast clones, we did not detect fMet-tRNA$^{Met}$, and interestingly, the KO clones showed preferential accumulation of the aminoacylated Met-tRNA$^{Met}$ with two of three mutant clones showing lower levels of deacylated tRNA$^{Met}$ (Fig. 2, *A* and *B*). We observed a marked increase of total mitochondrial tRNA$^{Met}$ levels (Fig. 2*C*), similar to previous results in humans (9). These results indicate that MTFMT is required for *N*-formylation of the Met-tRNA$^{Met}$ and suggest that the absence of MTFMT activity may affect the regulation of the tRNA$^{Met}$ ratios in mammalian mitochondria.

### *N*-Formylation is not an absolute requirement for mitochondrial protein synthesis in mammalian mitochondria

To evaluate the effects of MTFMT absence on mitochondrial protein synthesis, we measured the metabolic incorporation of radiolabeled [$^{35}$S]Met-Cys in the 13 mitochondrially encoded proteins in the presence of an irreversible inhibitor of cytoplasmic ribosomes (emetine). Using a short pulse (15–30 min), we observed the synthesis of all 13 mitochondrially encoded proteins in the *Mtfmt*-KO cell clones relative to *Mtfmt* controls (Fig. 3*A*). Interestingly, the rate of synthesis varied among the individual subunits (Fig. 3*C*). It was drastically reduced for ND4 (83%) followed by subunits ND4L (59%), COI (57%), ND6 (56%), ND1 (53%), and COIII (47%). It was not significantly altered for subunits CYTB (35%), COII/ATP6 (33%), ND3 (20%), and ATP8 (130%). ND5 and ND2 subunits from complex I were not detected, suggesting that both proteins have a low rate of synthesis in this fibroblast cell model as they could be observed in pulse-chase experiments (Fig. S2). The ND1 subunit not only showed a decreased rate of synthesis in the *Mtfmt*-KO clones but also faster migration relative to control cells (Fig. 3*B*, *enlarged panel*). We did not detect this migration difference in two different mouse cell models of complex I deficiency (*Ndufs3*-KO) and complex IV deficiency (*Cox10*-KO) (Fig. S1), which indicates that the absence of *N*-formylation not only affects the rate of synthesis but has an additional effect on the electrophoretic mobility of this subunit. The lack of specific antibodies made it difficult to address this question as we could not isolate ND1 to sequence the N terminus.

Altogether, these results demonstrated that, in mammals, mitochondrial protein synthesis occurs in the absence of *N*-formylation. However, lack of *N*-formylation compromised the efficiency of synthesis of the 13 mitochondrially encoded polypeptides to different degrees.

### Absence of *N*-formylation does not have a marked effect in the stability of mitochondrially encoded polypeptides

We then wanted to investigate whether the absence of *N*-formylation has any effect on the stability of the newly synthesized mitochondrially encoded polypeptides. For that, we determined the rate of degradation of each polypeptide in the *Mtfmt*-KO cell clones relative to controls using the pulse-chase radiolabeling assay and measuring the rate of [$^{35}$S]Met-Cys incorporation at two different chase times (9 and 18 h). In this assay, cells were pretreated with chloramphenicol (a reversible mitochondrial protein synthesis inhibitor) for 24 h, which results in the accumulation of the nuclearly encoded components required for mitochondrial protein synthesis.

Pulse labeling with [$^{35}$S]Met-Cys detected all mitochondrially encoded polypeptides, including subunits ND5 and ND2 in the *Mtfmt*-KO cells, confirming the synthesis of both subunits in the absence of *N*-formylation (Fig. S2). After a 9-h chase, the rate of degradation as well as the turnover in *Mtfmt* control cells varied among the individual subunits. ND5 subunit was no longer detected at 9 h, most likely due to the fast turnover rate compared with the other subunits. This was followed by sub-

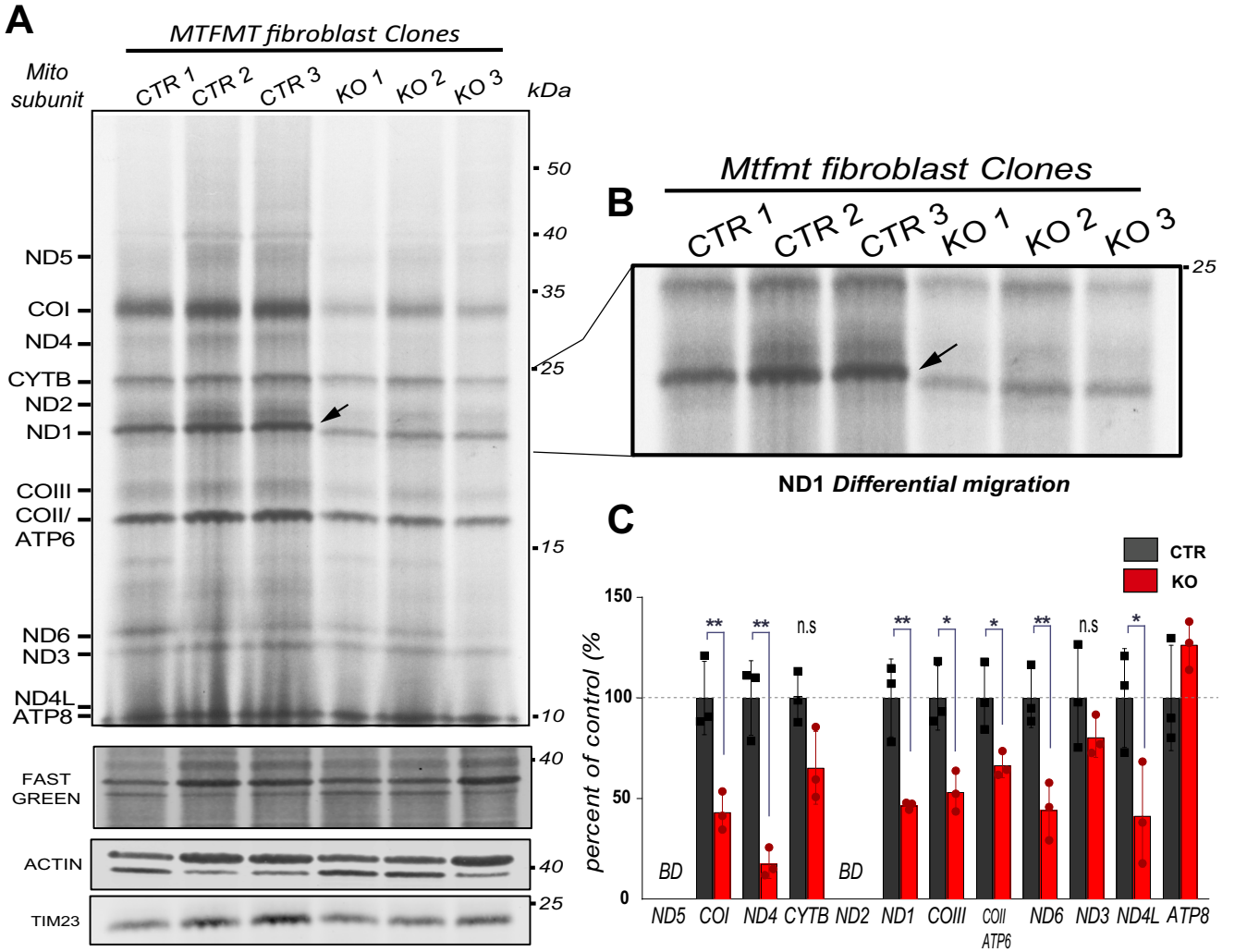


**Figure 3. Mitochondrial protein synthesis in *Mtfmt*-KO fibroblast clones occurs in the absence of *N*-formylation.** *A*, representative pattern of a [$^{35}$S]Met-Cys–pulse-labeled mitochondrial translation (30 min) in the presence of emetine as a cytoplasmic protein synthesis inhibitor. Fast green staining was used as a total loading protein control, β-actin was used as a cytoplasmic control, and TIM23 was used as a mitochondrial control. *B*, absence of *N*-formylation in the *Mtfmt*-KO cells resulted in faster migration of the ND1 (*black arrowhead*). *C*, individual rates of mitochondrial protein synthesis of *Mtfmt*-KO cells (*red*) expressed as percentage of control (*black*) and normalized to fast green staining. Data from three independent short pulse experiments (three clones each)) are presented as the mean, and *error bars* represent ±S.D. Two-way ANOVA with Bonferroni correction was used to compare each subunit (*, $p < 0.05$; **, $p < 0.01$). *BD*, below detection; *n.s.*, not significant. COII and ATP6 have the same expected size and were quantified as one band.

units ND2, ND3, and ND4L, which were detected at lower intensity, suggesting that the turnover of this group of proteins is quicker compared with the other remaining subunits (Fig. S2). The rate of degradation in *Mtfmt*-KO cells relative to controls was determined as the percent decrease of [$^{35}$S]Met-Cys–incorporated label from the pulse time point (0.5 h) (Fig. 4). We found that, although the stability of the ATP8 subunit decreased in the *Mtfmt*-KO cells at 9-h chase ($p < 0.01$) and the stability of the ND4 subunit had a trend to decrease in *Mtfmt*-KO cells, the remaining subunits had very similar rates of degradation. We validated these results by measuring and comparing the rate of degradation in our model with the rate of degradation in *bona fide* complex I- and IV-deficient cell models (Fig. S3). We found that the stability of certain subunits was highly compromised and varied depending on the model studied (Figs. S4 and S5), which confirms that the absence of *N*-formylation does not have a major effect on the stability of the mitochondrially encoded proteins.

### *Absence of N-formylation affects the steady-state levels of OXPHOS complexes*

We tested whether the lack of MTFMT, either by reduced efficiency of synthesis of the mitochondrially encoded subunits or by any other mechanism, has an effect on the steady-state level of OXPHOS components. We measured the steady-state levels of different mitochondrial markers by immunoblotting (Fig. 5) and found that NDUFB8, a late-stage subunit during the assembly of complex I, decreased in the *Mtfmt*-KO cells ($p < 0.007$), whereas NDUFA9, an early-stage assembly subunit of the hydrophilic arm of complex I, did not.

Steady-state levels of COIV, a nuclearly encoded subunit essential for assembly of complex IV, was markedly decreased ($p < 0.006$) in the *Mtfmt*-KO cells. We did not detect significant changes in the steady-state levels of COI; succinate dehydrogenase complex flavoprotein subunit A (SDHA), a catalytic subunit of complex II; ubiquinol-cytochrome *c* reductase core pro-

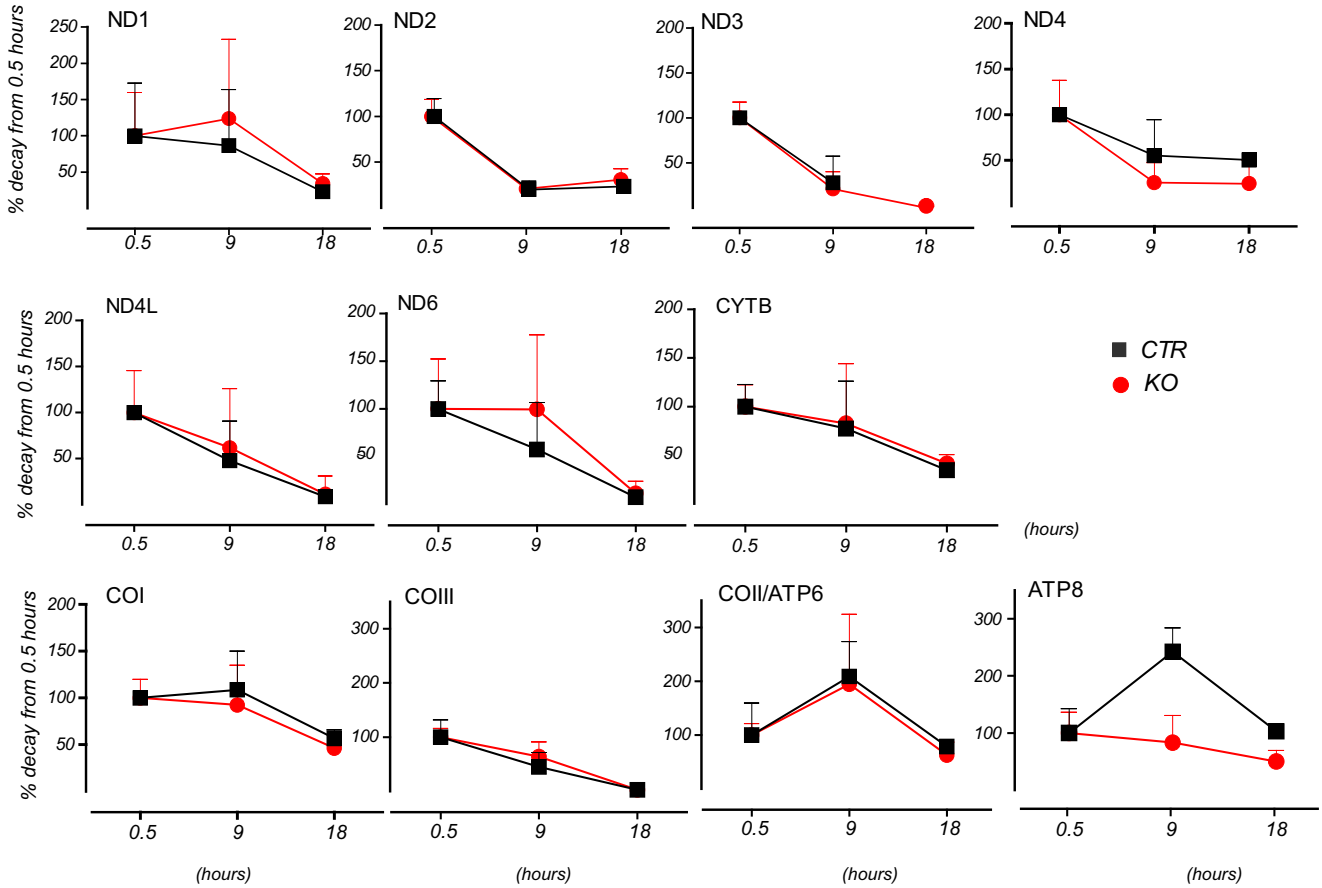


**Figure 4. Absence of *N*-formylation does not affect the stability of newly synthesized subunits in the first 18 h.** The rate of degradation of each polypeptide in the *Mtfmt*-KO cells was measured as percentage of decay from [$^{35}$S]Met-Cys incorporation at 30 min (pulse, 0.5 h) in the presence of anisomycin (a reversible cytosolic protein synthesis inhibitor) followed by chase at 9 and 18 h. There were no major changes in the stability of the mitochondrially synthesized polypeptides. ATP8 levels were increased at 9 h in controls ($p < 0.01$). Results are expressed as the mean (*error bars* represent ±S.D.) of three different cell clones (CTR in *black*; KO in *red*);. Ponceau staining and fast green staining were used as loading controls. Two-way ANOVA was used for analyses. ND3 was not detected at 18 h, and COII and ATP6 have the same expected size and were quantified as one band.

tein I (UQCRC1), a core subunit component of complex III; and ATP synthase subunit α (ATP5A), a subunit of complex V.

### *Absence of N-formylation affects preferentially complexes I and IV and assembly into supercomplexes*

We then analyzed the assembly of the individual OXPHOS complexes and their interactions into supercomplexes. We detected these macrocomplexes using blue native polyacrylamide gel electrophoresis (BN-PAGE) after solubilization with digitonin. In *Mtfmt* control cells, the majority of detected complex I was preferentially assembled into the respirasome structure corresponding to the CI–$CIII_2$–$CIV_n$ form and the supercomplex CI–$CIII_2$ with a small portion still detected in the isolated CI form. In contrast, in the *Mtfmt*-KO clone cells, there was a significant decrease of total complex I (70%) with the presence of CI–$CIII_2$ but no detectable levels of CI–$CIII_2$–$CIV_n$ or free CI (Fig. 6, *A* and *B*), indicating that the absence of *N*-formylation had profound consequences to complex I levels and its association into supercomplexes.

In the case of complex III, *Mtfmt* control cells showed preferential association into supercomplexes CI–$CIII_2$–$CIV_n$ and CI–$CIII_2$ with low levels of free complex III. In the *Mtfmt*-KO cells, complex III instead was lost from the CI–$CIII_2$–$CIV_n$ but was highly increased in the free and CI–$CIII_2$ forms. The levels of complex IV decreased by 60% in the *Mtfmt*-KO cells, whereas total complex II levels showed a significant increase, possibly as a compensatory mechanism. Analysis of complex V did not show any change in the *Mtfmt*-KO cells; however, there was a slight increase in the nonmembrane-embedded module termed F1. Altogether, these results indicate that the absence of *N*-formylation affects preferentially the assembly of individual complexes I and IV and the supercomplex interactions, mostly in the CI–$CIII_2$–$CIV_n$ form. We also evaluated the activity of the individual complexes I and IV and supercomplexes using BN-PAGE in-gel activity and found a pattern of activity nearly identical, indicating that disruption of OXPHOS complex assembly correlates with the observed decrease in activity of individual complexes I and IV at complex and supercomplex levels (Fig. 6*C*).

### *Absence of N-formylation results in increased glycolysis rate in Mtfmt-KO cells*

To identify the physiologic effects of MTFMT absence in mitochondrial and cellular bioenergetics, we measured the oxygen consumption rate (OCR) and extracellular acidification rate (ECAR) in *Mtfmt*-KO intact cells and compared them with controls using the XFp extracellular flux analyzer (Seahorse Biosciences).

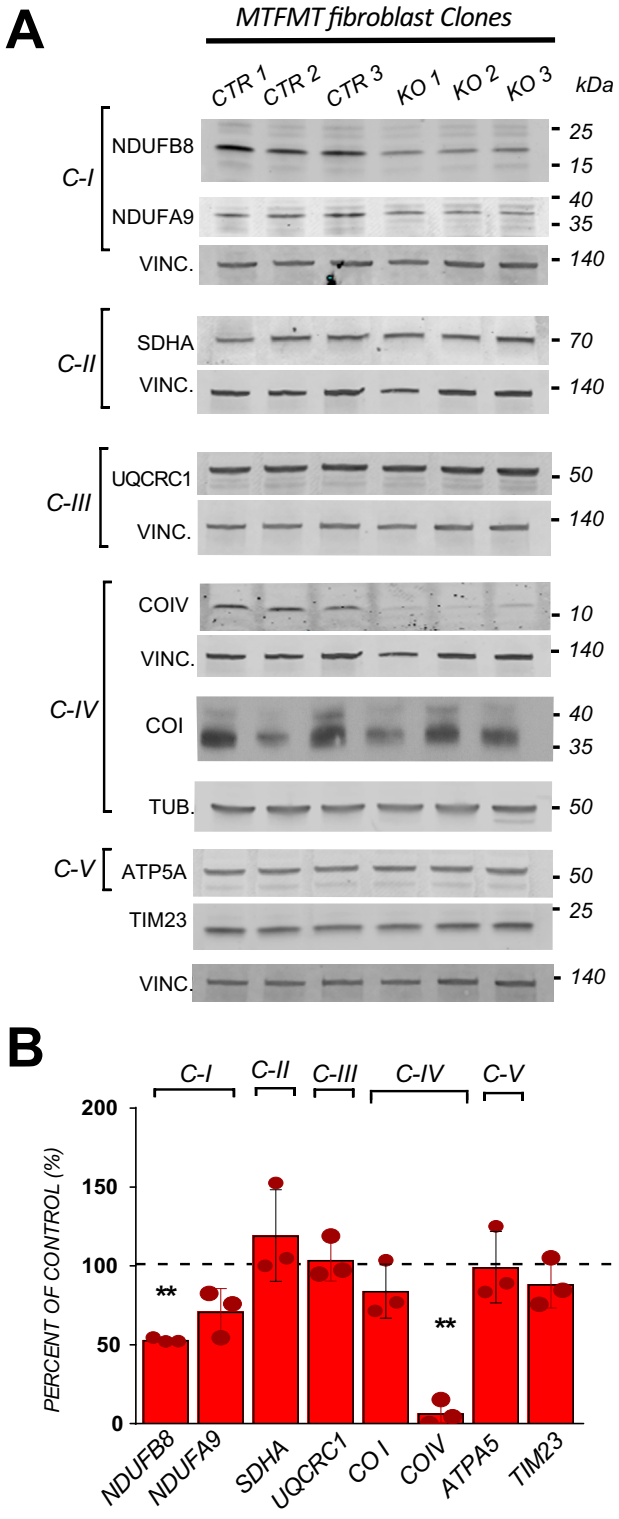


**Figure 5. Absence of *N*-formylation affects the steady-state levels of OXPHOS complexes.** *A*, representative Western blots from total protein lysates show decreased levels of NDUFB8 subunit (**, $p < 0.007$) of complex I (*C-I*) and COIV (**, $p < 0.006$) of complex IV (*C-IV*) in *Mtfmt*-KO cells. No significant changes were observed in other OXPHOS markers. *B*, values are expressed as a percentage of CTR and represent the mean (*error bars* represent ±S.D.) of three independent experiments (three clones each) for NDUFB8, NDUFA9, and COI or three clones for the other markers. Vinculin (*VINC.*) and tubulin (*TUB.*) were used as loading controls. Vinculin blots were the same for CIV and SDHA, NDUFA9 and NDUFB8; TIM23 and ATP5A, and UQCRC1. Tubulin was the loading control for COI. Two-tailed *t* test was used for statistical analyses.

Basal respiration was decreased by 22% in the *Mtfmt*-KO cells (Fig. 7*A*). ATP-linked respiration did not change nor did maximal respiratory capacity (Fig. S6A). Consequently, spare respiratory capacity (OCR difference between the basal and maximal respiratory capacities) increased by 59%. Although we cannot explain the unaltered maximum respiration, the increase in spare respiratory capacity could be a consequence of alternative substrate utilization under uncoupled conditions in the KO cells.

Conversely, basal glycolysis in the *Mtfmt*-KO cells increased by 40% ($p = 0.0055$) (Figs. 7*B* and S6). Subsequent addition of oligomycin to inhibit ATP from oxidative phosphorylation did not change the glycolytic capacity of KO cells relative to control. There was a 38% decrease in glycolytic reserve (Fig. 7*B*), reflecting the adaptation of *Mtfmt*-KO cells to glycolysis.

## Discussion

*N*-Formylation of Met-tRNA$^{Met}$ by the MTFMT enzyme is an exclusive mechanism of mitochondrial protein synthesis in eukaryotes. However, in mammals, the absolute requirement of *N*-formylation to start mitochondrial protein synthesis is still debated. In this study, we generated a *Mtfmt*-KO mouse fibroblast cell clone model, deleting exon 4 of the *Mtfmt* gene, which in humans harbors the most frequent pathogenic allele, c.626C→T. We confirmed the complete deletion of exon 4 at the DNA level and did not detect the MTFMT protein, demonstrating the generation of *Mtfmt*-KO mouse cell lines. Because this region is required for activity (16, 18), its ablation leads to the formation of a null allele as confirmed by our findings. The availability of a complete KO allowed us to study the role of MTFMT in a well defined genetic background.

Initially, we observed that *N*-formylation of the mitochondrial Met-tRNA$^{Met}$ was lacking in the *Mtfmt*-KO fibroblast clones, confirming that MTFMT is required for *N*-formylation of the Met-tRNA$^{Met}$ in mouse mitochondria. Our analysis of the tRNA ratios indicated that, in mouse fibroblast control cells, the three forms of mitochondrial tRNA$^{Met}$ are maintained at approximately equal ratios. Studies with human fibroblasts showed preferential accumulation of the *N*-formylated and deacylated forms (9). However, the significance of this variation is unknown. It is generally accepted that only a portion of the unique Met-tRNA$^{Met}$ inside mitochondria is *N*-formylated as fMet-tRNA is needed only for initiation. However, it is not known how these ratios are regulated and how they affect mitochondrial protein synthesis. Tucker *et al.* (9) reasoned that, in human fibroblasts, the low levels of Met-tRNA$^{Met}$ could be a result of its rapid use during the elongation process. In contrast, in mouse, the aminoacylated tRNA$^{Met}$ proportion remains at levels that are similar to the other tRNA$^{Met}$ forms. Interestingly, in mutated *MTFMT* patient cells and in the mouse *Mtfmt*-KO cells, the absence of *N*-formylation results in a preferential accumulation of the aminoacylated tRNA$^{Met}$ and an overall increase of total tRNA$^{Met}$, potentially as a compensatory mechanism. There were differences in ratios between aminoacylated and deacylated tRNA$^{Met}$ among the different *Mtfmt*-KO cells, but it is not known what caused these differences. This study also demonstrated that mitochondrial protein synthesis occurs in the absence of *N*-formylation of the mitochondrial

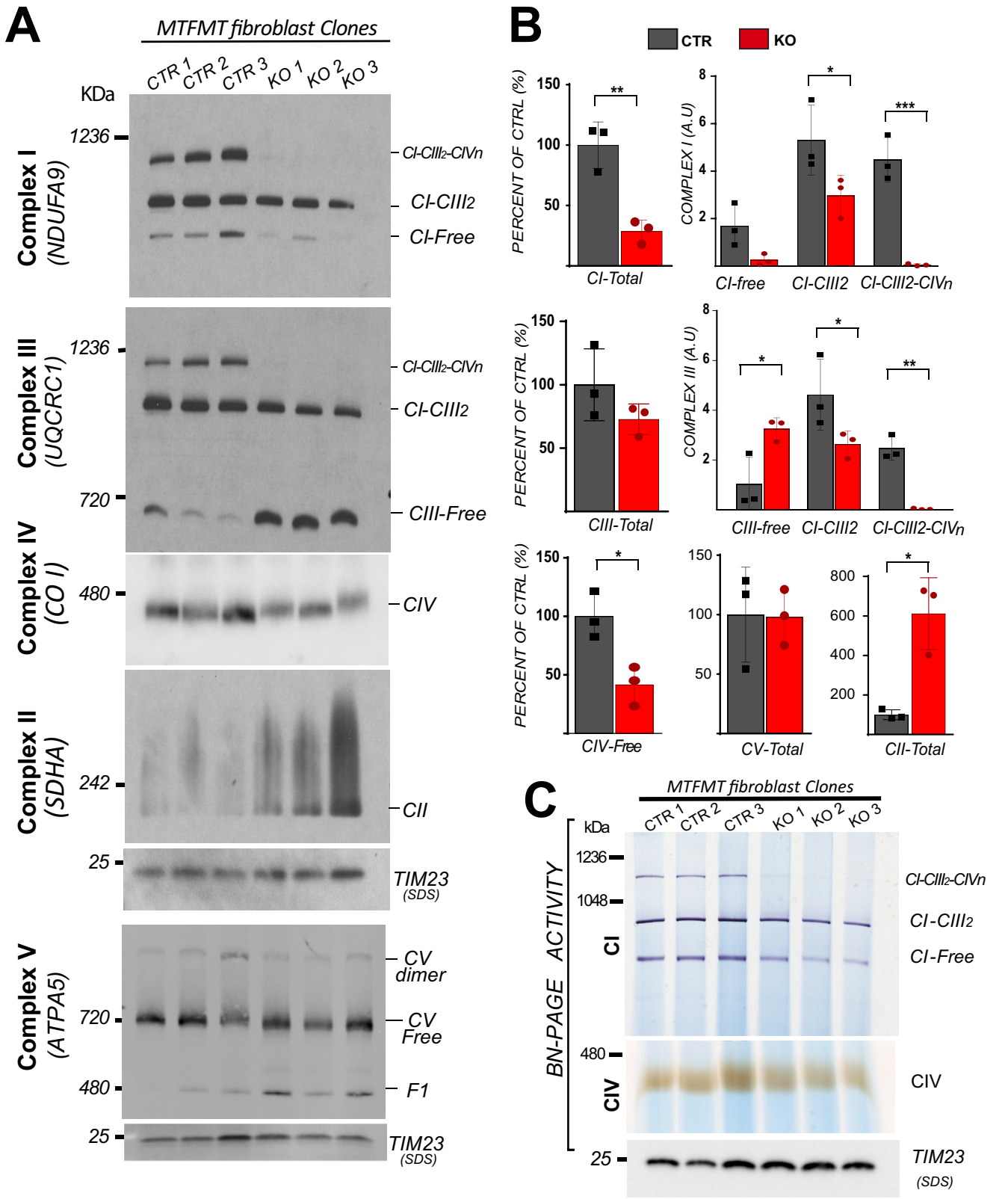


**Figure 6. Absence of *N*-formylation affects assembly of complexes I and IV and supercomplexes.** *A*, analysis of OXPHOS complex and supercomplex assembly was done by BN-PAGE in the presence of digitonin followed by Western analyses using the antibodies in *parentheses* to identify each complex. Note the nearly absent CI–$CIII_2$–$CIV_n$ supercomplex and decreases in complexes I and IV. All values were normalized to TIM23; *F1*, ATP synthase F1 complex. *B*, data are presented as the mean (*error bars* represent ±S.D.) of three clones, and unpaired two-way ANOVA was used for statistics (*, $p < 0.05$; **, $p < 0.01$; ***, $p < 0.001$). Total levels of complexes I, II, III, IV, and V were analyzed using unpaired two-tailed Student's *t* test. *C*, BN-PAGE in-gel activity showed decreased activity of free CI and supercomplexes (CI–$CIII_2$ and CI–$CIII_2$–$CIV_n$) in *Mtfmt*-KO cells and decreased free CIV activity. TIM23 was used as a loading control. *CTRL*, control.

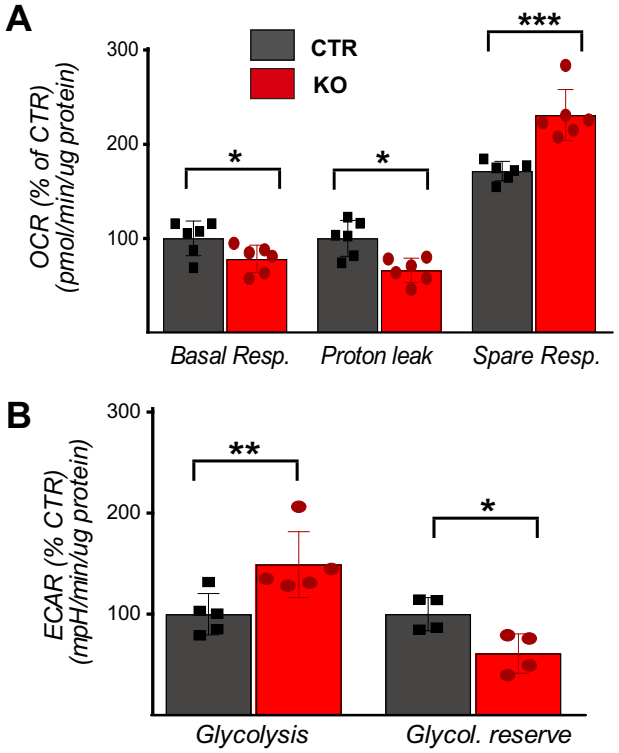


**Figure 7. Absence of *N*-formylation results in increase of glycolysis rate in *Mtfmt*-KO cells.** *A*, mitochondrial respiration rate of *Mtfmt*-KO intact cells measured using the OCR and expressed as percentage of control showed decreased basal respiration (*Resp.*) (*, $p < 0.0469$), mitochondrial proton-leak respiration (*, $p < 0.022$) (calculated as the OCR difference after the addition of oligomycin and rotenone/antimycin), and increased spare respiratory capacity (***, $p < 0.0005$) (measured as the difference between maximal respiration, OCR after addition of fluoro-carbonyl cyanide phenylhydrazone, and basal respiration). *B*, measurements of glycolytic function in *Mtfmt*-KO cells using the ECAR showed increased basal glycolysis (**, $p < 0.005$) and decreased glycolytic (*Glycol.*) reserve (*$p < 0.022$) (calculated as the difference between the basal glycolysis after adding glucose and the glycolytic capacity after addition of oligomycin). Data are presented as the mean (*error bars* represent ±S.D.), analyzed using unpaired two-tailed Student's *t* test. $n = 6$ independent experiments for OCR and $n = 5$ (CTR) and $n = 4$ (KO) for ECAR (three technical replicates each).

Met-tRNA$^{Met}$, which indicates that *N*-formylation of the Met-tRNA$^{Met}$ is not an absolute requirement of mitochondrial protein synthesis in mammals, but instead *N*-formylation has a critical role in the efficiency of synthesis and possibly assembly of certain mitochondrially encoded proteins.

It is widely accepted that mitochondria are derived from bacteria, and, therefore not surprisingly, the mitochondrial translational machinery shares many features, including the *N*-formylation of the Met-tRNA$^{Met}$ to be used in initiation. One interesting evolutionary question is whether mitochondria continue to rely on *N*-formylation for protein synthesis or whether they can function without it. *N*-Formylation of Met-tRNA$^{Met}$ was already shown to be dispensable in certain bacteria, such as *P. aeruginosa* (7), and yeast (2), providing the first clue that, at least in lower eukaryotes, formylation of the mitochondrial initiator tRNA is not an absolute requirement. In mammals, bovine mitochondrial mtIF2 initiation factor strongly prefers *N*-formylated fMet-tRNA$^{Met}$ over nonformylated Met-tRNA$^{Met}$ (19, 20). Conversely, bovine mtIF2 also supports protein synthesis in yeast mutants without formylated initiator tRNA (21). Our data provide evidence that the mammalian mitochondrial translational machinery can function without MTFMT but not as efficiently.

Interestingly, in our mouse model, we found that the effect on the efficiency of synthesis is different for the various mitochondrially encoded polypeptides. In this model, the absence of *N*-formylation affected drastically the rate of synthesis of the ND4 subunit, but less of an effect for others (ND1, ND4L, ND6, COI, COII/ATP6, and COIII), and had no significant effects in the rates of CYTB, ATP8, and ND3 subunits. In humans, two other studies (13, 14) have reported a preferential rate of decrease for the subunits ND1, ND5, ND4, and COII. However, it is not known whether this differential susceptibility is species-specific, whether it correlates with the structural properties of each subunit during assembly, or whether it is connected to additional functional roles of N-terminal formylation of mitochondrially encoded proteins, such as the generation of *N*-formyl peptides. In humans, *N*-formylated hexapeptides such as ND4, ND6, and COI are agonists of formyl peptide receptor-1 and induce chemotactic cellular responses involved in the modulation of the immune response (22, 23).

We also observed a differential migration in the ND1 subunit in SDS gels. We excluded the effect of polymorphisms in this *Mtfmt*-KO mouse model, which have been considered to be a major source of differences in the electrophoretic migrations observed in pulse experiments (24, 25). Interestingly, by reviewing SDS gels in the literature, this differential migration pattern can also be observed in one of the patients (P1) with mutations in *MTFMT* (13). Despite our attempts, efforts in sequencing the N-terminal region of ND1 were unsuccessful, mostly because there are no effective antibodies against the mouse ND1 that allowed for immunoprecipitation and MS sequencing of the N terminus. We speculate that this change in molecular weight could reflect an alternative mechanism of synthesis in response to the absence of *N*-formylation, such as the use of an alternative start codon for initiation or other mechanism yet to be discovered. In fact, ND1 in mouse is the only subunit that uses GUG (coding for valine) as initiator instead of a canonical codon (AUN).

The absence of *N*-formylation did not cause a major effect on the stability of the mitochondrial subunits in the mouse *Mtfmt*-KO cells as demonstrated by the pulse-chase experiments at 9 and 18 h. However, we showed that the absence of *N*-formylation did affect preferentially the steady-state levels of individual complexes I and IV and drastically impacted the organization into the CI–CIII$_2$–CIV$_n$ supercomplex. Although this could be a simple consequence of decreased steady-state levels of mtDNA-coded subunits, it may also point to a role for *N*-formylation in complex assembly. The physiological role of supercomplexes is still debated, but destabilization of these supramolecular assemblies could reduce efficiency of ATP production in homeostasis or stress situations (26). The assembly of complex I was the most severely affected with ~70% total reduction in BN-PAGE and loss of the major supercomplex organization. Complex I has seven subunits translated in the mitochondria that are critical components of the proton translocation membrane arm. In the absence of *N*-formylation, at least two subunits, ND4 and ND1, showed lower levels or differential migration, respectively. There was also a decrease in

steady-state levels of the nuclearly encoded transmembrane helix NDUFB8, which was shown to interact with ND4 subunit during complex I assembly, suggesting that the *N*-formyl residue may have a role in the assembly process of these subunits into individual complexes, which consequently may affect their interaction and stability in supercomplexes.

Absence of *N*-formylation did not affect the total levels of complex III in the *Mtfmt*-KO cells, which correlated with the normal steady-state levels of the mitochondrial UQCRC1, a core subunit of complex III, and no changes in efficiency of synthesis of the only mitochondrially encoded complex III subunit, CYTB. However, there was a marked effect in the supramolecular organization of this complex. In the absence of *N*-formylation, complex III accumulated preferentially in the free form with reduction of CI–$CIII_2$ association and loss of the major CI–$CIII_2$–$CIV_n$ supercomplex. Complex III has been shown to be required for stability of complex I (27) and to be preferentially organized into the CI–$CIII_2$ supercomplex under normal physiological conditions (28), which suggest that these changes in supercomplex organization could result primarily from the drastic decrease of complex I.

Complex IV, in contrast, showed 60% decreased levels in the absence of *N*-formylation, which correlated with the significant decrease in efficiency of *de novo* protein synthesis of mitochondrially encoded subunits COI and COIII and the drastic decrease in steady-state levels of the nuclearly encoded COIV, an assembly factor of complex IV, indicating an important role of *N*-formylation not only in the assembly/stability of this individual complex but also in the drastic effects on the major CI–$CIII_2$–$CIV_n$ supercomplex association.

It is still unclear whether *N*-formylation contributes to the structural stability of the supramolecular structure. Electrospray ionization MS in bovine heart mitochondria identified that, with the exception of the COIII subunit, all 12 mitochondrially encoded proteins retain the *N*-formyl group (29). Studies of complex IV assembly in patient fibroblasts with mutations in MTFMT have shown a severe decrease in *N*-formylated COI in the assembled complex IV, indicating that the *N*-formyl residue of the COI may facilitate assembly into the complex (13). However, in a previous study, *N*-formylated COI was detected as the most abundant form in two patient fibroblasts with mutations in MTFMT (9). Although it is not known what caused these contrasting differences, further studies in the mouse model should help elucidate the effects of the absence of *N*-formylation in complex IV assembly and correlate them with the human counterpart.

Assembly/stability of individual complex V was not affected in absence of *N*-formylation, which correlated with no changes in the steady-state levels of the mitochondrial membrane ATP5A. The increased levels of ATP8 from complex V also showed normal rate levels, which indicates that the absence of *N*-formylation does not have a major effect on the mitochondrially encoded subunit part of these complexes.

The functional implications of the absence of *N*-formylation in the *Mtfmt*-KO mouse model were reflected by the reduction of activity of individual complex I and complex IV and the levels of the major CI–$CIII_2$–$CIV_n$ respirasome. These likely explain the decrease of the basal mitochondrial respiration rate and the switch to glycolysis to maintain the overall energy demand. This suggests a metabolic adaptation of the *Mtfmt*-KO cells and a compromised ability to respond to stress. This is also in agreement with the lactic acidosis observed in patients with Leigh syndrome and *MTFMT* mutations and could provide insights into the clinical variability and onset of the disease (10, 12).

In summary, we have generated *Mtfmt*-KO fibroblast mouse cell lines and confirmed that *N*-formylation is not an absolute requirement for mitochondrial protein synthesis in mice; however, it is critical for efficiency of synthesis of certain mitochondrially encoded subunits. Absence of *N*-formylation does not affect stability of the *de novo* synthesized subunits but instead affects drastically the assembly/stability of complexes I and IV, which has profound effects on their association into supercomplexes. The absence of *N*-formylation results in increased reliance on glycolysis for energy production. Although cultured fibroblasts showed normal growth and survival without MTFMT, it is possible that *N*-formylation is critical for optimal OXPHOS function in specific tissues or stress situations. Future experiments with animal models will help answer these questions.

## Experimental procedures

### *Generation of the ex vivo Mtfmt knockout cell model*

Dermal fibroblasts were derived from skin tissue explants from 3-month adult homozygous $Mtfmt^{loxP/loxP}$ mice followed by immortalization and transfection with the CMV cre recombinase (cre) plasmid as described elsewhere (17). Confirmation of successful recombination using cre transgene expression *ex vivo* was done by amplifying the putative deleted region in the *Mtfmt* gene after cre recombinase activity by short PCR using specific primers. DNA was extracted from the parental $Mtfmt^{loxP/loxP}$ clone and *Mtfmt*-KO clone cells.

### *Cell culture conditions*

Mouse fibroblast $Mtfmt^{loxP/loxP}$ controls and *Mtfmt*-KO cells were grown in T 75-$cm^2$ cell culture flasks using high-glucose DMEM supplemented with fetal bovine serum (15%; Sigma), sodium pyruvate (1 mM), nonessential amino acids (1×), uridine (0.1 mg/ml), and gentamicin (20 mg/ml; all obtained from Gibco). Cells were maintained at 37 °C and 5% $CO_2$. *Mtfmt* control cells were used between passages 30 and 50, and *Mtfmt*-KO cells were used between passages 20 and 30. Other controls used in these experiments, such as the mouse fibroblast cell line NIH3T3, were grown in the same cell culture conditions. All the cells used in the study were tested for *Mycoplasma* contamination by PCR. Control (CTR) clones 1–3 were selected after immortalization. KO clones 1–3 were derived from the same parental clone, identified as CTR 2. The same controls and knockouts are shown consistently throughout the study.

### *Mitochondrial extraction*

Mitochondrially enriched fractions were obtained by a nitrogen cavitation method with slight modifications from Gottlieb and Adachi (30). In brief, cells were grown to 90% confluence and collected using 0.05% trypsin, EDTA (Gibco). The pellet

was washed in cavitation buffer A (100 mM sucrose, 1 mM EGTA, 20 mM MOPS, pH 7.4, 1 g/liter BSA) (Sigma). The new pellet obtained was resuspended in cavitation buffer B (cavitation buffer A plus 10 mM triethanolamine and 5% (w/v) Percoll (Sigma) supplemented with protein inhibitor mixture (Roche Applied Science)) and placed in the cavitation vessel. Cell disruption was achieved using nitrogen gas to 600 p.s.i. and allowed to equilibrate for 30 min. Cells were collected by differential centrifugation (2500 and 15,000 rpm) to separate the crude mitochondrial pellet and stored at −80 °C.

### *Mitochondrial translation assays*

Cells were grown to 90% confluence in 6-well plates. Mitochondrial protein synthesis was performed in L-methionine-L-cysteine–free DMEM (1×) supplemented with dialyzed fetal bovine serum (10%) and sodium pyruvate (1 mM) from Gibco. Cells were incubated for 10 min with emetine (100 $\mu$g/ml) as an irreversible cytoplasmic protein inhibitor during the pulse experiments and with anisomycin (100 $\mu$g/ml) as a reversible cytoplasmic protein inhibitor during chase experiments. For the chase experiments only, cells were pretreated with chloramphenicol (40 $\mu$g/ml) for 24 h. All reagents were obtained from Sigma.

Approximately 400 $\mu$Ci/ml EXPRESS$^{35}$S methionine-cysteine protein labeling mixture (PerkinElmer Life Sciences) was added to the medium, and the radioisotope labeling was performed for at least 15–30 min. This followed a short incubation of 5 min with DMEM supplemented with fetal bovine serum (10%) and sodium pyruvate (1 mM) prior to cell collection. For the chase experiments, cells were metabolically labeled for 30 min (pulse) and chased at two time points (9 and 18 h). Protein extraction was performed using radioimmune precipitation assay buffer followed by quantification using the DC Protein Assay kit (Bio-Rad). Approximately 40–50 $\mu$g was loaded onto an SDS-polyacrylamide 17.5% gel (30% acrylamide, 0.2% bisacrylamide) (5% stacking gel). The running buffer (1×) was adjusted to pH 8.3 before use, and the gel was run at 100 V for ~15–17 h. Transfer was performed using nitrocellulose membranes (Bio-Rad) and the Owl$^{TM}$ HEP Series Semidry Electroblotting System for at least 3 h. The membrane was dried and exposed to film for at least 4 days. Quantification of bands was done using optiQuant software (PerkinElmer Life Sciences). Fast green FCF (0.002%) followed by scanning at 625 nm using the Odyssey IR Imaging System (LI-COR Biosciences) or Ponceau staining was used as total protein loading controls.

### *SDS-PAGE and immunoblotting*

Steady-state protein levels were measured in mitochondrially enriched fraction as described previously or in total protein homogenates. Approximately 20–40 $\mu$g of protein was mixed with Laemmli buffer (Bio-Rad) supplemented with 5% mercaptoethanol and denatured for 15 min at 65 °C. Samples were separated on 4–20 or 10% SDS-polyacrylamide gels and transferred to polyvinylidene difluoride membranes. Membranes were blocked with 5% milk in 0.1% Tween 20, PBS (PBST) for 1 h and subsequently incubated with specific primary antibodies overnight at 4 °C. The antibodies used included goat polyclonal to MTFMT (T-12) at 1:500 obtained from Santa Cruz Biotechnology (sc-137618), rabbit anti-actin at 1:1000 from Sigma, (A2006), and mouse anti-TIM23 at 1:1000 BD Biosciences (611222). From Abcam, we used mouse monoclonal to MTCO1 at 1:1000 (ab14705), mouse monoclonal to ATP5A at 1:1000 (ab14748), mouse monoclonal to NDUFA9 at 1:1000 (ab14713), mouse monoclonal to SDHA at 1:1000 (ab14715), mouse monoclonal to NDUFB8 at 1:1000 (ab110242), mouse monoclonal to UQCRC1 at 1:2000 (ab110252), mouse monoclonal to COIV at 1:2000 (ab33985), and mouse monoclonal to vinculin at 1:5000 (ab18058).

Secondary antibodies used were horseradish peroxidase–conjugated anti-mouse at 1:5000, anti-rabbit at 1:3000, and anti-goat at 1:5000 (Santa Cruz Biotechnology) or IRDye 800–conjugated anti-mouse IgG (610-732-124) and IRDye 700–conjugated anti-rabbit IgG (610-430-002) (Rockland). Signal was detected by chemiluminescence using the Super Signal West Pico reagent or by scanning using the Odyssey IR Imaging System.

### *BN-PAGE analysis*

BN-PAGE analysis was performed as described previously (31). Approximately four T-75 flasks were grown to 90% confluence. Cell pellets were collected after trypsin digestion. Membrane dissolution was carried out by addition of 8 mg/ml digitonin (Sigma), and recovered pellets were resuspended in aminocaproic buffer (1.5 M aminocaproic acid and 50 mM Bis-Tris) containing protease inhibitors. Approximately 100 $\mu$g of protein was resuspended in aminocaproic buffer and treated with digitonin at a 1:8 ratio (protein:digitonin) (Calbiotech) for 20 min. Recovered supernatant was mixed with 0.5% SERVA Blue G dye (5% SERVA Blue G (w/v), 0.5 mM EDTA, 50 mM Bis-Tris, 750 mM aminocaproic buffer) before loading. 15–30 $\mu$g was loaded on a gel. BN-PAGE was carried out in precast 3–12% Bis-Tris blue native gels (Invitrogen). 1× blue cathode buffer (10 mM Tricine, 3 mM Bis-Tris-Cl, pH 7.0, 0.004% (w/v) SERVA Blue G dye) was used to fill the inner chamber, and 1× anode fuffer (50 mM Bis-Tris, pH 7.0) was used for the outer chamber. Samples were run at 100 V for 1 h at 4 °C after which the 1× blue cathode buffer was replaced with 1× colorless cathode buffer (10 mM Tricine, 3 mM Bis-Tris-Cl, pH 7.0), and the gel was run at 8 mA for 4 h. Gels were transferred to polyvinylidene difluoride membranes overnight at 75 V at 4 °C. Membranes were dried at 37 °C for 15 min followed by rehydration with methanol. Membrane blocking was carried out in 5% milk in PBST for 4 h before immunoblotting.

### *Acid-urea PAGE and Northern blot analysis*

Acid-urea PAGE and preparation of samples were performed according to Köhrer and Rajbhandary (32) with slight modifications. In brief, cells were grown in a T150 flask to 90% confluence. Cell pellets were collected after trypsin digestion. For total RNA extraction, the cell pellet was resuspended in TRIzol (Invitrogen), 1/10 volume of sodium acetate buffer (0.3 M sodium acetate, pH 4.5–5.0, 10 mM $Na_2EDTA$) and acid-washed glass beads (0.5-mm diameter; Sigma) were added, and RNA was extracted following Invitrogen's instructions for TRIzol. The RNA was precipitated with ethanol and recovered by centrifugation at 12,000 × *g* for 15 min at 4 °C, and the pellet was

washed twice with 70% ethanol; finally dissolved in 20–50 μl of 10 mM sodium acetate, pH 4.5–5.0; and stored at −80 °C until further use. Aminoacyl-tRNAs and formyl aminoacyl-tRNAs were deacylated by base treatment (alkaline treatment) in 0.1 M Tris-HCl, pH 9.5, at 65 °C for 5 min followed by incubation at 37 °C for 1 h. Aminoacyl-tRNAs were selectively deacylated by treatment with copper sulfate as described (33). Treated RNAs from *Mtfmt* control and *Mtfmt*-KO cells were separated by acid-urea PAGE as described previously with modifications (9). Briefly, 0.1 $A_{260}$ unit of each RNA sample was loaded onto a 6.5% polyacrylamide gel containing 7 M urea and 0.2 M sodium acetate, pH 5.0. The gel was run in the cold room at 500 V (~12 V/cm) for ~70 h. Individual tRNAs were detected by Northern blotting using the following hybridization probes: 5′-TAGTACGGGAAGGGTATAA-3′ (mitochondrial $tRNA^{Met}$) and 5′-TTCCACTGCACCACTCTGCT-3′ (cytoplasmic initiator $tRNA_i^{Met}$). Northern blot images were quantified using Image Studio™ Lite software (LI-COR Biosciences).

### Mitochondrial bioenergetics

Approximately $2 \times 10^5$ cells were seeded in a Seahorse culture plate (3 wells/cell line), and incubated in a 37 °C in a 5% $CO_2$ humidified atmosphere for 24 h. The cell culture medium from the cell plates was replaced the following day with 175 μl/well prewarmed low-buffered serum-free Seahorse medium supplemented with glutamine (2 mM), sodium pyruvate (1 mM), and glucose (10 mM) and incubated at 37 °C in a $CO_2$-free incubator for 45 min to allow the temperature and pH of the medium to reach equilibrium before the first rate measurement. The pH of the medium was then adjusted to 7.4 with 1 M NaOH. For the mitochondrial respiration rate, the OCR was analyzed in response to oligomycin (1 μM), fluoro-carbonyl cyanide phenylhydrazone (1 μM), and rotenone plus antimycin A (all Sigma) (1 μM). The oxygen consumption rate was used to determined basal respiration, ATP-linked respiration, proton leak, maximum respiratory capacity, spare respiratory capacity, and non-mitochondrial respiration. For the glycolysis assay, the ECAR was measured by monitoring changes in pH in intact cells after sequential addition of glucose (10 mM), oligomycin (1 μM), and the inhibitor of the hexokinase 2-deoxy-D-glucose (75 mM). We measured glycolysis and glycolytic capacity after the addition of oligomycin and estimated the glycolytic reserve as well as the nonglycolytic acidification after the addition of 2-deoxy-D-glucose. All calculations were performed according to the manufacturer's parameter guidelines. Measurement of protein concentration was performed at the end of each run to normalize OCR and ECAR by protein content using the Lowry assay (Bio-Rad).

### Activity in gel (BN-PAGE)

Approximately 60 μg of protein pretreated with mild digitonin were used for BN-PAGE as described above. For complex I activity, the gel was incubated in 0.1 M Tris-HCl, pH 7.4, containing 1 mg/ml nitro blue tetrazolium and 0.14 mM NADH at room temperature. For complex IV activity, the gel was incubated in 1.54 mM diaminobenzidine tetrahydrochloride dissolved in 50 mM phosphate buffer, pH 7.4. Both reactions were incubated at 37 °C for at least 30 min and stopped when the brown color for complex IV activity and blue-purple color for complex I activity appeared.

### Statistical analysis

Statistical significance was analyzed using GraphPad software. Two-way repeated-measures analysis of variance (ANOVA) followed by Bonferroni post hoc comparison was performed to analyze replicate means and evaluate interaction among the different technical experiments. Two-tailed unpaired Student's *t* test was also used to identify statistically significant differences between groups. $p < 0.05\%$ was considered significant. Experimental results are shown as mean ± S.D.

*Author contributions*—T. A. and C. T. M. conceptualization; T. A., C. K., U. L. R., and C. T. M. formal analysis; T. A., C. K., and U. L. R. investigation; T. A. and U. L. R. methodology; T. A. and C. T. M. writing-original draft; T. A. and C. T. M. project administration; T. A., C. K., U. L. R., and C. T. M. writing-review and editing; U. L. R. and C. T. M. supervision; C. T. M. funding acquisition.

## References


1. Christian, B. E., and Spremulli, L. L. (2012) Mechanism of protein biosynthesis in mammalian mitochondria. *Biochim. Biophys. Acta* **1819,** 1035–1054 CrossRef Medline
2. Kuzmenko, A., Atkinson, G. C., Levitskii, S., Zenkin, N., Tenson, T., Hauryliuk, V., and Kamenski, P. (2014) Mitochondrial translation initiation machinery: conservation and diversification. *Biochimie* **100,** 132–140 CrossRef Medline
3. RajBhandary, U. L. (1994) Initiator transfer RNAs. *J. Bacteriol.* **176,** 547–552 CrossRef Medline
4. Mai, N., Chrzanowska-Lightowlers, Z. M., and Lightowlers, R. N. (2017) The process of mammalian mitochondrial protein synthesis. *Cell Tissue Res.* **367,** 5–20 CrossRef Medline
5. Guillon, J. M., Mechulam, Y., Schmitter, J. M., Blanquet, S., and Fayat, G. (1992) Disruption of the gene for Met-tRNA(fMet) formyltransferase severely impairs growth of *Escherichia coli*. *J. Bacteriol.* **174,** 4294–4301 CrossRef Medline
6. Vanunu, M., Lang, Z., and Barkan, D. (2017) The gene *fmt*, encoding tRNA(fMet)-formyl transferase, is essential for normal growth of *M. bovis*, but not for viability. *Sci. Rep.* **7,** 15161 CrossRef Medline
7. Newton, D. T., Creuzenet, C., and Mangroo, D. (1999) Formylation is not essential for initiation of protein synthesis in all eubacteria. *J. Biol. Chem.* **274,** 22143–22146 CrossRef Medline
8. Li, Y., Holmes, W. B., Appling, D. R., and RajBhandary, U. L. (2000) Initiation of protein synthesis in *Saccharomyces cerevisiae* mitochondria without formylation of the initiator tRNA. *J. Bacteriol.* **182,** 2886–2892 CrossRef Medline
9. Tucker, E. J., Hershman, S. G., Köhrer, C., Belcher-Timme, C. A., Patel, J., Goldberger, O. A., Christodoulou, J., Silberstein, J. M., McKenzie, M., Ryan, M. T., Compton, A. G., Jaffe, J. D., Carr, S. A., Calvo, S. E., RajBhandary, U. L., *et al.* (2011) Mutations in MTFMT underlie a human disorder of formylation causing impaired mitochondrial translation. *Cell Metab.* **14,** 428–434 CrossRef Medline
10. Haack, T. B., Gorza, M., Danhauser, K., Mayr, J. A., Haberberger, B., Wieland, T., Kremer, L., Strecker, V., Graf, E., Memari, Y., Ahting, U., Kopajtich, R., Wortmann, S. B., Rodenburg, R. J., Kotzaeridou, U., *et al.* (2014) Phenotypic spectrum of eleven patients and five novel MTFMT mutations identified by exome sequencing and candidate gene screening. *Mol. Genet. Metab.* **111,** 342–352 CrossRef Medline
11. Haack, T. B., Haberberger, B., Frisch, E. M., Wieland, T., Iuso, A., Gorza, M., Strecker, V., Graf, E., Mayr, J. A., Herberg, U., Hennermann, J. B., Klopstock, T., Kuhn, K. A., Ahting, U., Sperl, W., *et al.* (2012) Molecular diagnosis in mitochondrial complex I deficiency using exome sequencing. *J. Med. Genet.* **49,** 277–283 CrossRef Medline

12. Neeve, V. C., Pyle, A., Boczonadi, V., Gomez-Duran, A., Griffin, H., Santibanez-Koref, M., Gaiser, U., Bauer, P., Tzschach, A., Chinnery, P. F., and Horvath, R. (2013) Clinical and functional characterisation of the combined respiratory chain defect in two sisters due to autosomal recessive mutations in MTFMT. *Mitochondrion* **13,** 743–748 CrossRef Medline
13. Hinttala, R., Sasarman, F., Nishimura, T., Antonicka, H., Brunel-Guitton, C., Schwartzentruber, J., Fahiminiya, S., Majewski, J., Faubert, D., Ostergaard, E., Smeitink, J. A., and Shoubridge, E. A. (2015) An N-terminal formyl methionine on COX 1 is required for the assembly of cytochrome c oxidase. *Hum. Mol. Genet.* **24,** 4103–4113 CrossRef Medline
14. La Piana, R., Weraarpachai, W., Ospina, L. H., Tetreault, M., Majewski, J., Care4Rare Canada Consortium, Bruce Pike, G., Decarie, J. C., Tampieri, D., Brais, B., and Shoubridge, E. A. (2017) Identification and functional characterization of a novel MTFMT mutation associated with selective vulnerability of the visual pathway and a mild neurological phenotype. *Neurogenetics* **18,** 97–103 CrossRef Medline
15. Oates, A., Brennan, J., Slavotinek, A., Alsadah, A., Chow, D., and Lee, M. M. (2016) Challenges managing end-stage renal disease and kidney transplantation in a child with MTFMT mutation and moyamoya disease. *Pediatr. Transplant.* **20,** 1000–1003 CrossRef Medline
16. Sinha, A., Köhrer, C., Weber, M. H., Masuda, I., Mootha, V. K., Hou, Y. M., and RajBhandary, U. L. (2014) Biochemical characterization of pathogenic mutations in human mitochondrial methionyl-tRNA formyltransferase. *J. Biol. Chem.* **289,** 32729–32741 CrossRef Medline
17. Arguello, T., and Moraes, C. T. (2015) Cre recombinase activity is inhibited in vivo but not ex vivo by a mutation in the asymmetric spacer region of the distal loxP site. *Genesis* **53,** 695–700 CrossRef Medline
18. Takeuchi, N., Kawakami, M., Omori, A., Ueda, T., Spremulli, L. L., and Watanabe, K. (1998) Mammalian mitochondrial methionyl-tRNA transformylase from bovine liver. Purification, characterization, and gene structure. *J. Biol. Chem.* **273,** 15085–15090 CrossRef Medline
19. Liao, H. X., and Spremulli, L. L. (1991) Initiation of protein synthesis in animal mitochondria. Purification and characterization of translational initiation factor 2. *J. Biol. Chem.* **266,** 20714–20719 Medline
20. Spencer, A. C., and Spremulli, L. L. (2004) Interaction of mitochondrial initiation factor 2 with mitochondrial fMet-tRNA. *Nucleic Acids Res.* **32,** 5464–5470 CrossRef Medline
21. Tibbetts, A. S., Oesterlin, L., Chan, S. Y., Kramer, G., Hardesty, B., and Appling, D. R. (2003) Mammalian mitochondrial initiation factor 2 supports yeast mitochondrial translation without formylated initiator tRNA. *J. Biol. Chem.* **278,** 31774–31780 CrossRef Medline
22. Krysko, D. V., Agostinis, P., Krysko, O., Garg, A. D., Bachert, C., Lambrecht, B. N., and Vandenabeele, P. (2011) Emerging role of damage-associated molecular patterns derived from mitochondria in inflammation. *Trends Immunol.* **32,** 157–164 CrossRef Medline
23. Rabiet, M. J., Huet, E., and Boulay, F. (2005) Human mitochondria-derived N-formylated peptides are novel agonists equally active on FPR and FPRL1, while *Listeria monocytogenes*-derived peptides preferentially activate FPR. *Eur. J. Immunol.* **35,** 2486–2495 CrossRef Medline
24. Sasarman, F., and Shoubridge, E. A. (2012) Radioactive labeling of mitochondrial translation products in cultured cells. *Methods Mol. Biol.* **837,** 207–217 CrossRef Medline
25. Fernández-Silva, P., Acín-Pérez, R., Fernández-Vizarra, E., Pérez-Martos, A., and Enriquez, J. A. (2007) *In vivo* and *in organello* analyses of mitochondrial translation. *Methods Cell Biol.* **80,** 571–588 CrossRef Medline
26. Acin-Perez, R., and Enriquez, J. A. (2014) The function of the respiratory supercomplexes: the plasticity model. *Biochim. Biophys. Acta* **1837,** 444–450 CrossRef Medline
27. Acín-Pérez, R., Bayona-Bafaluy, M. P., Fernández-Silva, P., Moreno-Loshuertos, R., Pérez-Martos, A., Bruno, C., Moraes, C. T., and Enríquez, J. A. (2004) Respiratory complex III is required to maintain complex I in mammalian mitochondria. *Mol. Cell* **13,** 805–815 CrossRef Medline
28. Acín-Pérez, R., Fernández-Silva, P., Peleato, M. L., Pérez-Martos, A., and Enriquez, J. A. (2008) Respiratory active mitochondrial supercomplexes. *Mol. Cell* **32,** 529–539 CrossRef Medline
29. Walker, J. E., Carroll, J., Altman, M. C., and Fearnley, I. M. (2009) Chapter 6 Mass spectrometric characterization of the thirteen subunits of bovine respiratory complexes that are encoded in mitochondrial DNA. *Methods Enzymol.* **456,** 111–131 CrossRef Medline
30. Gottlieb, R. A., and Adachi, S. (2000) Nitrogen cavitation for cell disruption to obtain mitochondria from cultured cells. *Methods Enzymol.* **322,** 213–221 CrossRef Medline
31. Diaz, F., Barrientos, A., and Fontanesi, F. (2009) Evaluation of the mitochondrial respiratory chain and oxidative phosphorylation system using blue native gel electrophoresis. *Curr. Protoc. Hum. Genet.* **Chapter 19,** Unit 19.4 CrossRef Medline
32. Köhrer, C., and Rajbhandary, U. L. (2008) The many applications of acid urea polyacrylamide gel electrophoresis to studies of tRNAs and aminoacyl-tRNA synthetases. *Methods* **44,** 129–138 CrossRef Medline
33. Schofield, P., and Zamecnik, P. C. (1968) Cupric ion catalysis in hydrolysis of aminoacyl-tRNA. *Biochim. Biophys. Acta* **155,** 410–416 CrossRef Medline